Available online at www.sciencedirect.com
ScienceDirect
Journal of Physics and Chemistry of Solids 69 (2008) 1869–1876
JOURNAL OF PHYSICS AND CHEMISTRY OF SOLIDS
www.elsevier.com/locate/jpcs

Thermodynamic and kinetic properties of $Ho_{1-x}Ti_xCo_2$-hydrogen system

G. Srinivas[a,b], V. Sankaranarayanan[a], S. Ramaprabhu[b,*]

[a]Low Temperature Laboratory, Department of Physics, Indian Institute of Technology Madras, Chennai 600 036, India
[b]Alternative Energy Technology Laboratory, Department of Physics, Indian Institute of Technology Madras, Chennai 600 036, India

Received 24 April 2007; received in revised form 12 October 2007; accepted 15 November 2007

Abstract

The hydrogen absorption behavior of Laves phase $Ho_{1-x}Ti_xCo_2$ ($x = 0.1$–0.6) alloys has been investigated by pressure-concentration (PC) isotherms and cyclic-, temperature- and pressure-dependent absorption kinetics. The PC isotherms and kinetics of hydrogen absorption have been studied in the pressure range 0.01–1 bar and temperature range 50–200 °C using Sievert's-type apparatus. The drastic changes in the induction period and particle size during the activation process have been discussed based on the kinetics of repeated hydrogenation cycles and scanning electron microscopy (SEM) images of the hydrides at different hydriding cycles, respectively. The experimental results of kinetic curves are interpreted using the Johnson–Mehl–Avrami (JMA) model, and the reaction order and reaction rate have been determined. The α-, $(\alpha+\beta)$- and β-phase regions in $Ho_{1-x}Ti_xCo_2$-H have been identified from the different slope regions of the first-order-type kinetic plots. The dependence of the reaction rate parameter on hydriding pressure and temperature in the $(\alpha+\beta)$-phase region has been discussed.

Keywords: A. Intermetallic compounds; D. Phase transitions; D. Thermodynamic properties

1. Introduction

$RETM_2$ (RE = rare earth; TM = Mn, Fe, Co, Ni) Laves phase compounds easily absorb hydrogen and form stable hydrides [1–7]. There are very few reports on the thermodynamic and kinetic properties of these $RETM_2$-H, because of very low plateau pressures and complex behavior of hydrogen absorption and desorption properties [1–4]. The hydriding properties can be tuned by partial replacement or alloying with different kinds of elements [1,8–13]. Most of the hydrogen storage materials are of multielement alloys, and a lot of effort has been spent to optimize the materials for the best practical performance. However, much less importance has been given for fundamental understanding of the mechanism and kinetics of hydrogen absorption reaction. In order to understand hydride formation, the thermodynamic properties of the hydrides are very important. The kinetics of the metal hydrides has been investigated in order to map the reaction mechanisms of hydrogen absorption and desorption and to identify possible rate limiting steps to improve the kinetics. The reaction kinetics is greatly influenced by temperature and pressure but mostly, the hydriding–dehydriding kinetics are investigated with the influence of temperature in order to determine the reaction rate and mechanism [14,15]. Few investigations have been carried out on the effect of the initial hydrogen pressure of the system on the kinetics of hydrogen absorption [2,3,8,16–21]. In addition to temperature dependence of the reaction rate, the hydriding reaction strongly depends on the working pressure P of hydrogen, when the hydriding pressure is not too high relative to the equilibrium pressure P_{eq} of the hydride [3,8,22]. Recently, we have reported the structural and hydriding–dehydriding properties of Ti substituted $Ho_{1-x}Ti_xCo_2$-H system using powder X-ray diffraction (XRD), pressure-concentration (PC) isotherms, differential scanning calorimetry (DSC) and thermogravimetry (TG) studies [23–25]. The $Ho_{1-x}Ti_xCo_2$ alloys crystallize in single-phase cubic C15 Laves structure up to $x = 0.2$. The

*Corresponding author. Tel.: +91 44 22574862; fax: +91 44 22570509.
E-mail address: ramp@iitm.ac.in (S. Ramaprabhu).

0022-3697/$ - see front matter © 2007 Published by Elsevier Ltd.
doi:10.1016/j.jpcs.2007.11.016

formation of the secondary hexagonal C36 Laves structure is observed for $x>0.2$ and the amount of hexagonal to cubic Laves phase ratio increases with further increasing Ti substitution without much change in their lattice parameters. The variations in the hydrogen absorption plateau pressure and storage capacity have been discussed based on the change in the lattice parameter, formation of secondary hexagonal Laves phase structure and hydriding affinity of Ho and Ti. In the present study, we report the hydrogen absorption thermodynamic and kinetic properties of this Laves phase $Ho_{1-x}Ti_xCo_2$ alloys. The thermodynamic parameters have been obtained from the PC isotherms at different temperatures. The variations in the absorption kinetics during activation of the samples have been interpreted using the scanning electron microscopy (SEM) images of the hydrides. The influence of the hydriding pressure and temperature on the kinetics of activated samples has been analyzed and the dependence of rate parameter in the different hydride phase regions is discussed.

2. Experimental details

$Ho_{1-x}Ti_xCo_2$ ($x=0.1$–0.6) alloys were prepared by arc melting of stoichiometric amounts of constituent elements Ho, Ti and Co with a purity better than 99.9% under a protective argon atmosphere. The samples were repeatedly arc melted with the button being turned over. The weight loss during arc melting was <0.1 wt%. The ingots were annealed at 850 °C under vacuum for 72 h. The structural characterization of the $Ho_{1-x}Ti_xCo_2$ was carried out by powder XRD using an X'pert PRO, PANalytical diffractometer with nickel-filtered Cu Kα radiation under ambient air and scanning in the 2θ range of 15–90°, in steps of 0.05°. The homemade glass vacuum Sievert's-type experimental apparatus is used to obtain the PC isotherms and perform the hydrogen absorption kinetics. Annealed ingots of about 0.5 g were crushed to small pieces and introduced into the hydriding reactor. Before hydrogenation the system was flushed with hydrogen five or six times and was evacuated each time to $<10^{-5}$ mbar. The samples were activated by repeating hydrogen absorption and desorption cycles: (1) the absorption measurements have been carried out at 1 bar constant initial hydrogen pressure and temperatures at 100 and 150 °C, and (2) desorption carried out in a vacuum and temperature increases up to 800 °C. The absorption isotherm measurements were started with a completely desorbed sample. A controlled amount of hydrogen gas has been admitted into the reaction chamber that holds a specimen, and the pressure change has been monitored while maintaining constant temperature of the reaction chamber. The data points were obtained after reaching equilibrium pressure at each particular temperature. The amount of hydrogen absorbed was determined from the change in pressure measured at constant volume and temperature. The experiments for determining the reaction kinetics were performed at a specific temperature, which is kept constant to within ±1 °C, at various initial hydrogen pressures. The variation of the pressure of hydrogen in the known volume permits one to calculate the quantity of hydrogen absorbed by the sample as a function of time. The change in pressure in the hydriding reaction chamber with time is recorded until no more pressure change is detected and it is converted to the change in amount of hydrogen absorbed.

3. Results and discussion

3.1. Thermodynamic properties of hydrogen absorption

The thermodynamic parameters, the reaction enthalpy (ΔH_H) and the reaction entropy (ΔS_H) of $Ho_{1-x}Ti_xCo_2$-H have been calculated from temperature-dependent plateau pressure [23] using the van't Hoff equation:

$$\ln P_{eq} = 2\left(\frac{\Delta H_H}{RT} - \frac{\Delta S_H}{R}\right),$$

where T is the temperature in Kelvin and R is the universal gas constant. P_{eq} is the hydrogen absorption equilibrium

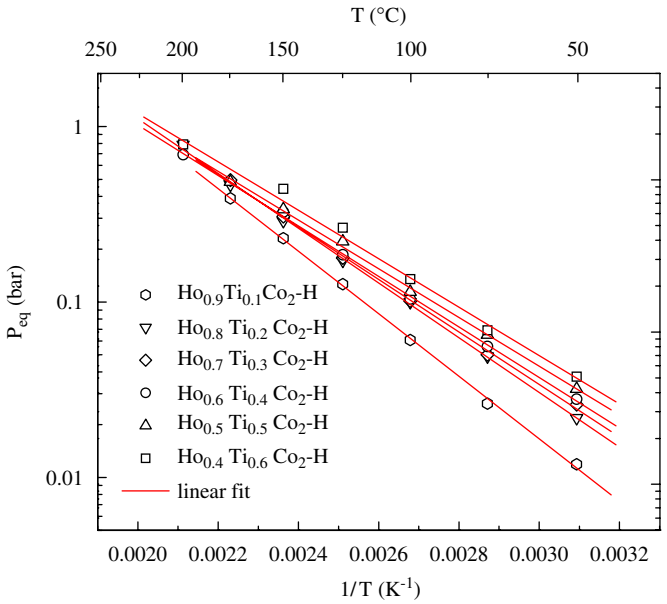

Fig. 1. van't Hoff plots of $Ho_{1-x}Ti_xCo_2$-H for $x=0.1$–0.6.

Table 1
The thermodynamic parameters of $Ho_{1-x}Ti_xCo_2$ ($x=0.1$–0.6) hydrides

Hydride composition	ΔH (kJ/mol-H)	ΔS (J/mol-H/K)
$Ho_{0.9}Ti_{0.1}Co_2$-H	−17.0(3)	−34(0.7)
$Ho_{0.8}Ti_{0.2}Co_2$-H	−14.9(2)	−30(0.5)
$Ho_{0.7}Ti_{0.3}Co_2$-H	−14.3(2)	−29(0.7)
$Ho_{0.6}Ti_{0.4}Co_2$-H	−13.8(2)	−28(0.5)
$Ho_{0.5}Ti_{0.5}Co_2$-H	−13.3(3)	−27(0.7)
$Ho_{0.4}Ti_{0.6}Co_2$-H	−13.0(5)	−27(0.7)

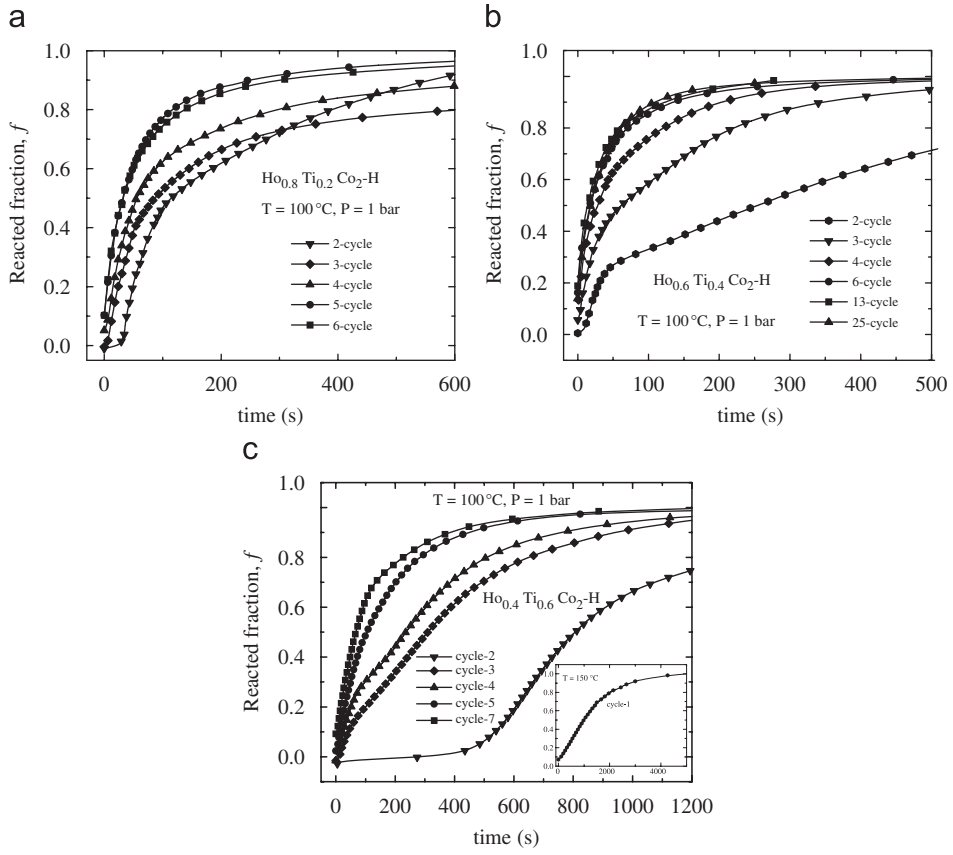

Fig. 2. Hydrogen absorption kinetic curves of (a) $Ho_{0.8}Ti_{0.2}Co_2$, (b) $Ho_{0.6}Ti_{0.4}Co_2$, and (c) $Ho_{0.4}Ti_{0.6}Co_2$, during activation with constant initial pressure of 1 bar and constant temperature of 100 °C; inset of (c) shows the complete kinetic plot of initial hydrogen absorption cycle for $Ho_{0.4}Ti_{0.6}Co_2$ at 1 bar and 150 °C.

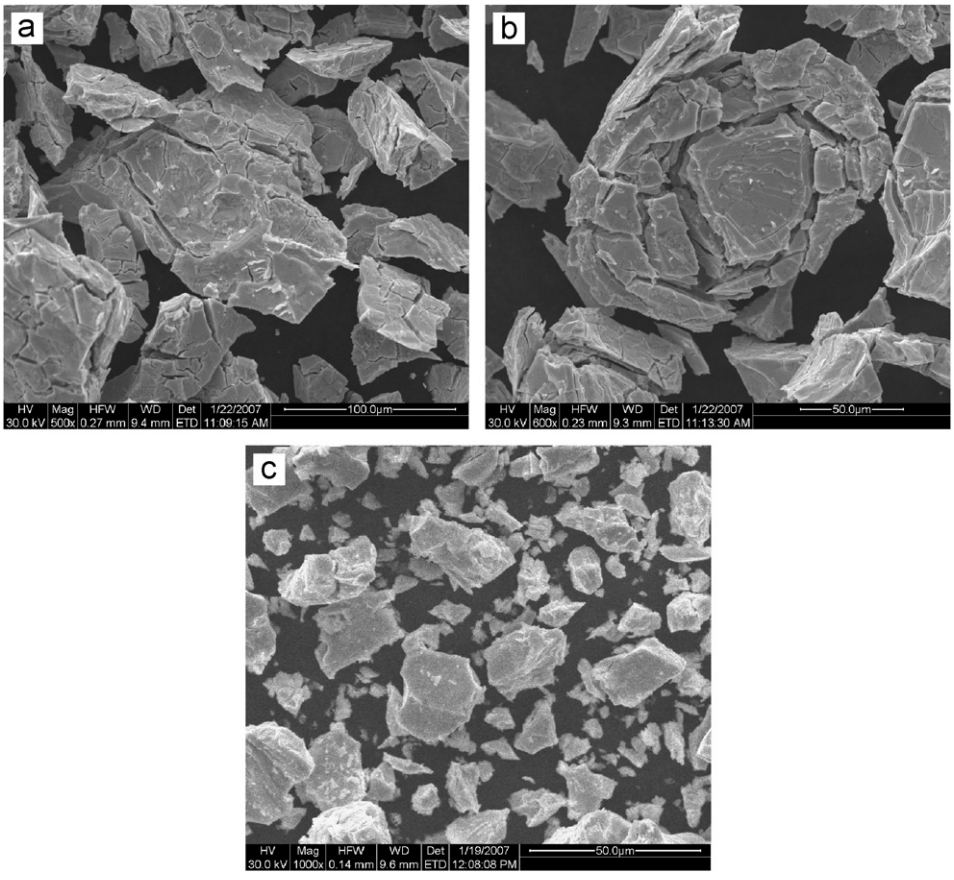

Fig. 3. SEM images of $Ho_{0.8}Ti_{0.2}Co_2$-hydrides: (a) and (b) after 1st cycle of hydrogenation and (c) after 3rd cycle of hydrogenation.

plateau pressure obtained from the center of the plateau region for each PC isotherm [4]. The van't Hoff plots of $Ho_{1-x}Ti_xCo_2$-H are shown in Fig. 1, the obtained ΔH_H and ΔS_H are listed in Table 1. The decrease in the magnitude of enthalpy in the function of x means that the stability of the hydrides decreases from $Ho_{0.9}Ti_{0.1}Co_2$-H to $Ho_{0.4}Ti_{0.6}Co_2$-H. From the previous reports on various types of alloy hydride systems [4,26–28], the hydride stability is interpreted in terms of their unit cell volume and interstitial hole size. The changes in the ΔS_H value are attributed to the partial substitution of Ti for Ho. The size and the nearest-neighbor arrangement of various interstitial sites might be varied due to the substitution. This may be the reason for the changing the magnitude of ΔS_H values.

3.2. Activation

Preliminary activation of hydrogen storage alloys is needed for their normal hydrogen absorption and desorption. The activation process consists of several repeated hydriding–dehydriding cycles, involves the following steps: (1) exposure to hydrogen (for absorbing hydrogen), (2) heating at high temperature in vacuum (for desorbing hydrogen) and (3) a series of absorption and desorption cycles. Fig. 2 shows the absorption kinetic curves plotted as reacted fraction, f vs. time at different number of hydriding cycles during activation for $Ho_{1-x}Ti_xCo_2$-H. The reacted fraction, f, is obtained from the ratio $f(t) = (P - P(t))/(P - P_\infty)$, where P is the initial pressure of the reaction. $P(t)$ and P_∞ are the pressures at time t and final

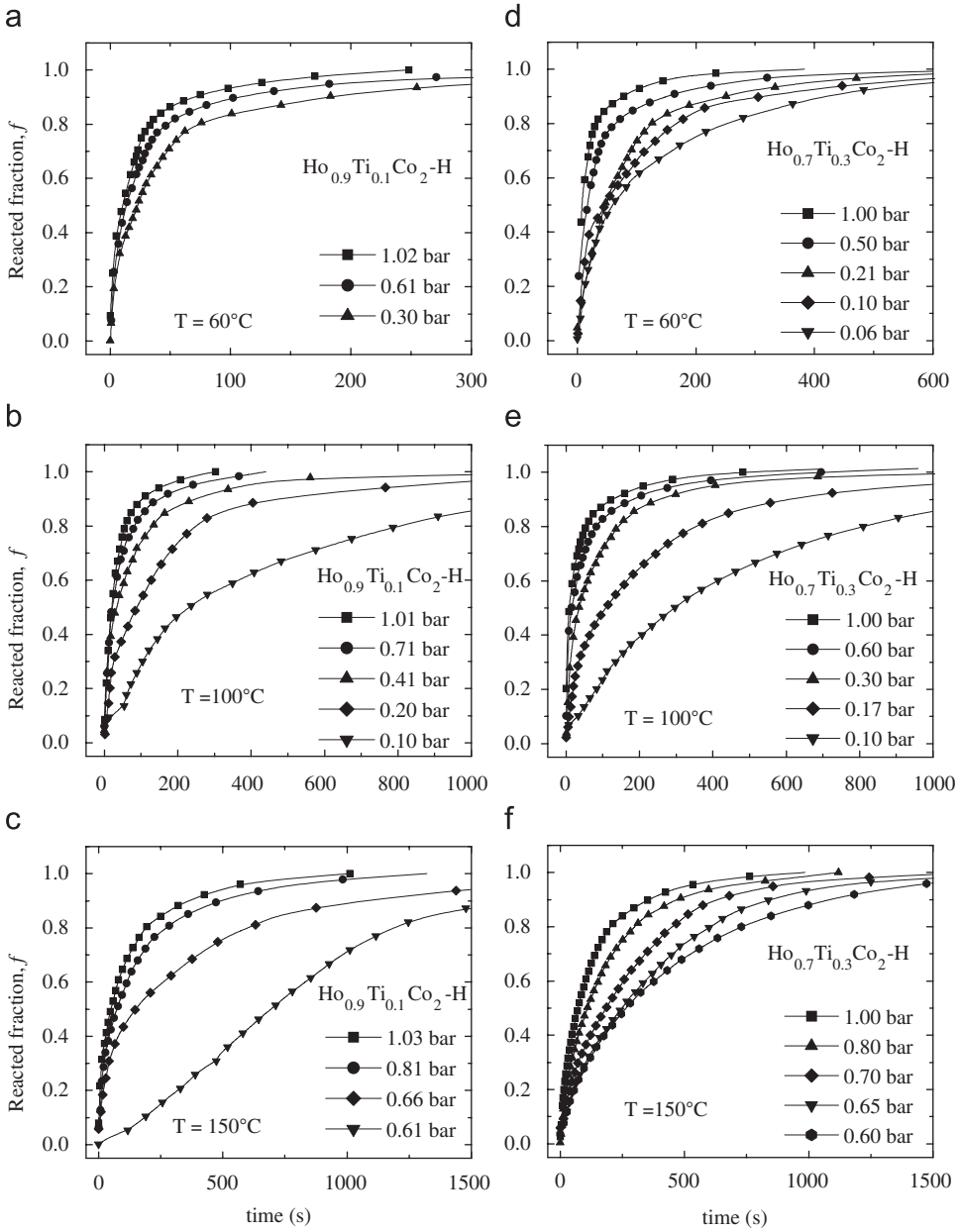

Fig. 4. Pressure-dependent kinetic plots (f vs. t) of activated $Ho_{0.9}Ti_{0.1}Co_2$-H and $Ho_{0.7}Ti_{0.3}Co_2$-H at different constant temperatures.

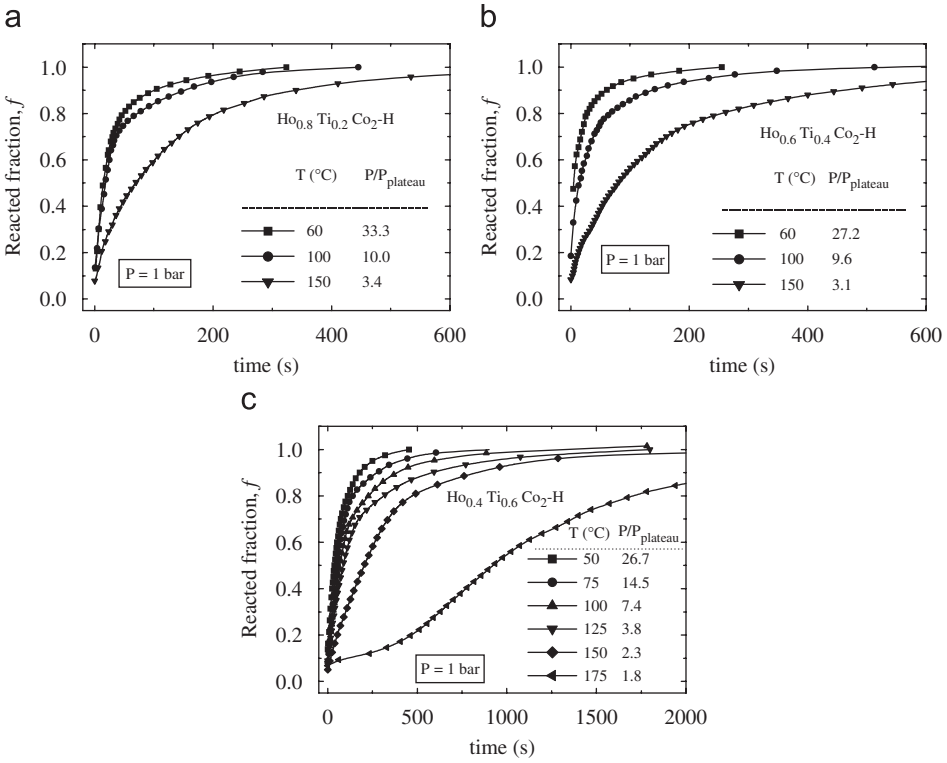

Fig. 5. Temperature-dependent activated kinetic plots (f vs. t) for (a) $Ho_{0.8}Ti_{0.2}Co_2$-H, (b) $Ho_{0.6}Ti_{0.4}Co_2$-H and (c) $Ho_{0.4}Ti_{0.6}Co_2$-H at constant initial hydrogen pressure of 1 bar.

equilibrium, respectively. These kinetic curves clearly demonstrate the changes observed with successive hydriding–dehydriding cycles. In the initial stage, an incubation period is followed by an accelerating stage, both of which become shorter as the number of cycles increases. In hydriding kinetics it is frequently observed that there is a sensible induction period until the reaction commences [3,29,30]. This appears to be generally due to surface oxides (or sulfides, nitrides, etc.) or to adsorbed gas, which inhibits hydriding until this layer is ruptured, reduced or permeated. The induction period drastically reduces with hydriding–dehydriding cycles due to disintegration of alloy into small particles and formation of new fresh surfaces [3,8,31]. The large volume expansion during hydride formation, the brittle nature of $Ho_{1-x}Ti_xCo_2$ alloys and plastic deformation lead to the formation of fine powder with fresh surfaces. Fig. 3 shows the SEM micrographs of $Ho_{0.8}Ti_{0.2}Co_2$-H, subjected to different hydriding cycles during activation. The vigorous breakage of the alloy particles can be seen by appearance of large number of microcracks in Figs. 3(a) and (b) just after a complete initial hydrogen absorption step. The formation of fine powders can be seen further repeating hydrogenation cycles (Fig. 3(c)). During the initial hydrogenation cycles the bulk alloy continuously decrepitates into smaller grains. However, this process continues for certain cycles, then after the grain size of the alloy remains unchanged for further repeated hydrogenation cycles. The fresh uncontaminated large surface area of smaller grains of alloy leads to the uniform hydrogen diffusion on the surface. Further

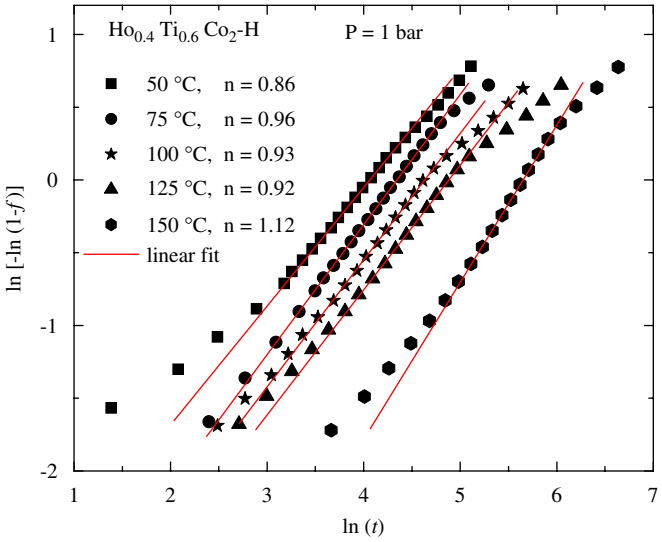

Fig. 6. $\ln[-\ln(1-f)]$ vs. $\ln(t)$ plots of $Ho_{0.4}Ti_{0.6}Co_2$-H at $P = 1$ bar with different hydriding temperatures.

the hydrogen absorption kinetics will be faster in the smaller grains due to smaller diffusion lengths for hydrogen.

3.3. Kinetics of hydrogen absorption: influence of pressure and temperature

Figs. 4 and 5 show the influence of the pressure and temperature on hydrogen absorption kinetics of some of

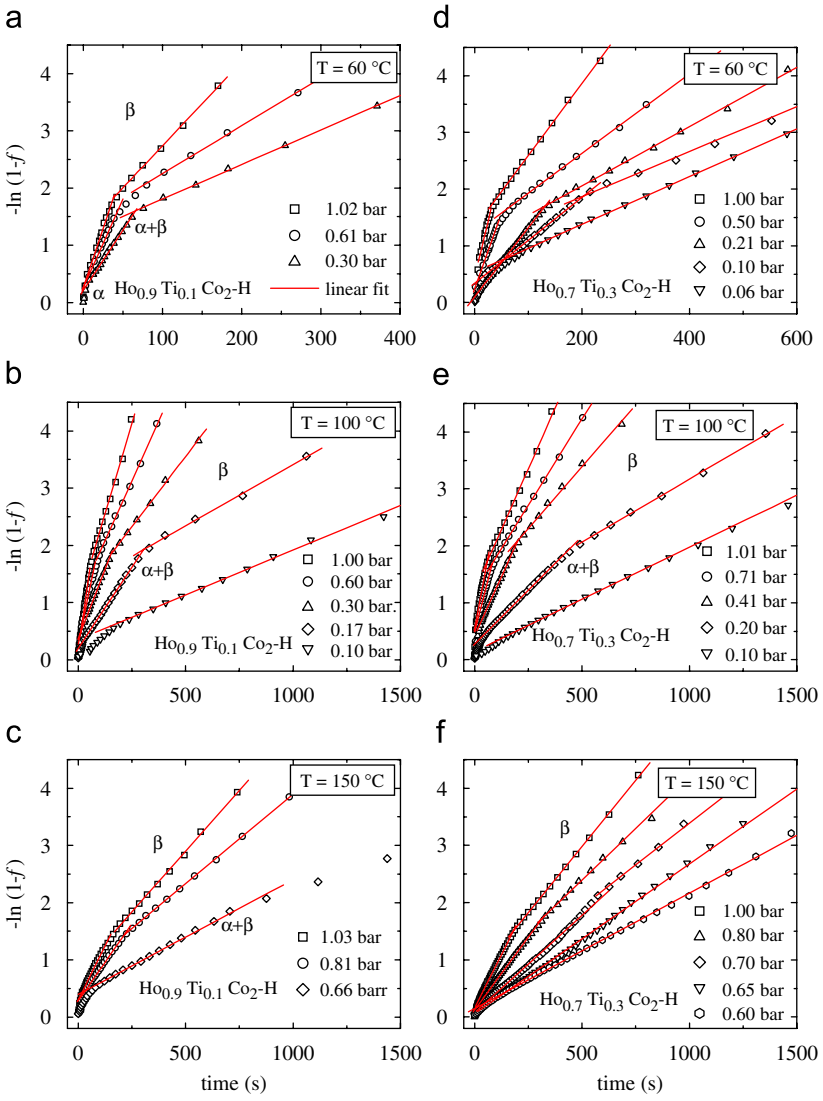

Fig. 7. Pressure-dependent first-order kinetic plots ($-\ln(1-f)$ vs. t) of $Ho_{0.9}Ti_{0.1}Co_2$-H and $Ho_{0.7}Ti_{0.3}Co_2$-H at different constant temperatures.

the activated $Ho_{1-x}Ti_xCo_2$ alloys. It can be seen from the qualitative behavior of kinetic plots in both the figures that the reaction rate decreased when decreasing hydriding pressure or increasing temperature. In order to get the proper reaction mechanism, reaction order and reaction rate parameters in different hydride phase regions, these kinetic plots are analyzed further by using the Johnson–Mehl–Avrami (JMA) theory [32], where the reacted fraction $f(t)$ is given as a function of time t, by

$$f(t) = 1 - \exp(-kt^n), \tag{1}$$

where $k = k(T)$ is the temperature-dependent rate parameter and n is the reaction order. Rearranging Eq. (1), we get

$$\ln[-\ln(1-f)] = n \ln t + \ln k. \tag{2}$$

Eq. (2) indicates that at a given temperature and pressure a plot of $\ln[-\ln(1-f)]$ vs. $\ln(t)$ is expected to be linear. The slope and intercept of a linear interpolation of the typical master plots, $\ln[-\ln(1-f)]$ vs. $\ln(t)$, yield the values of n and k, respectively. For example, Fig. 6 represents $\ln[-\ln(1-f)]$ vs. $\ln(t)$ plots for $Ho_{0.4}Ti_{0.6}Co_2$-H at $P = 1$ bar with different hydriding temperatures. A best linear fit of the experimental data in the $(\alpha+\beta)$-phase region gives the values of n very close to 1 ($n = 1 \pm 0.14$). Thus the reaction order indicates that the hydriding reactions are of first order. Therefore, the corresponding pressure- and temperature-dependent first-order plots ($-\ln(1-f)$ vs. t) of Figs. 4 and 5 are shown in Figs. 7 and 8, respectively. These first-order plots clearly demonstrate that almost in all the kinetic plots, each one consists of different linear segments, which extend in the certain range rather than linear over the entire reaction range. Each line segment represents a different stage in which the reaction is controlled by a different process [3,15,33–35]. These plots involve a phase transformation and demonstrate the existence of three phases, namely α-, $(\alpha+\beta)$- and β-phases, which are observed by the existence of different slopes of the straight-line segments and are changes at the phase boundary for each kinetic plot. In some cases, particularly

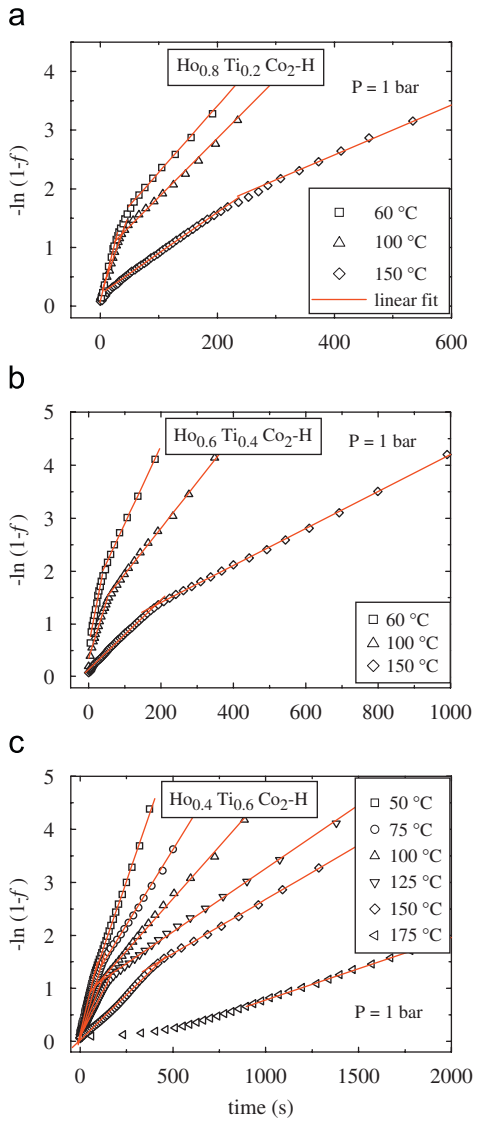

Fig. 8. Temperature-dependent first-order kinetic plots ($-\ln(1-f)$ vs. t) for (a) $Ho_{0.8}Ti_{0.2}Co_2$-H, (b) $Ho_{0.6}Ti_{0.4}Co_2$-H and (c) $Ho_{0.4}Ti_{0.6}Co_2$-H at constant initial hydrogen pressure of 1 bar.

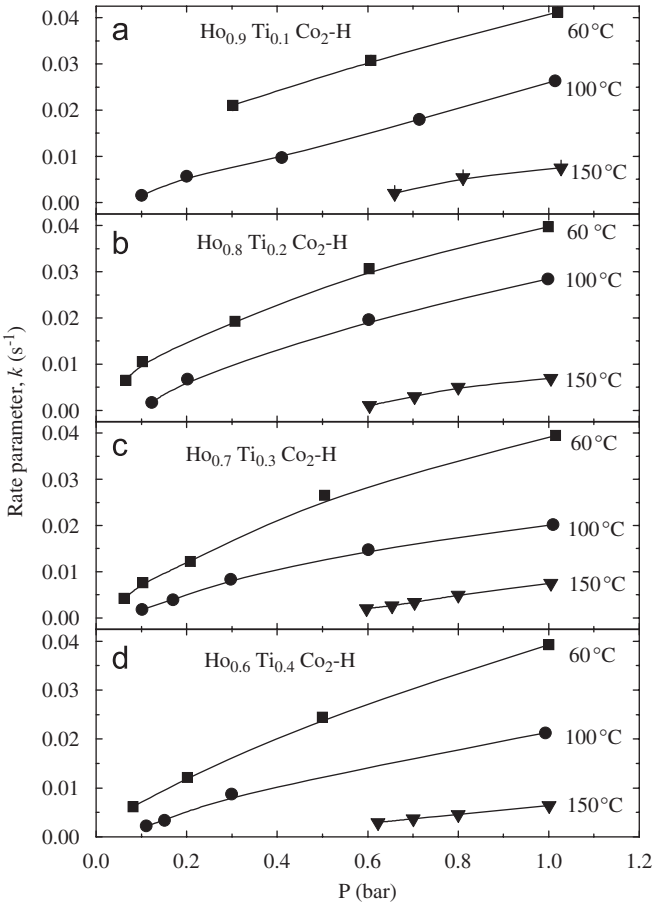

Fig. 9. Variation of rate parameter as a function of pressure in the $(\alpha+\beta)$-phase region for $Ho_{1-x}Ti_xCo_2$-H with $x = 0.1$–0.4 at different constant temperatures.

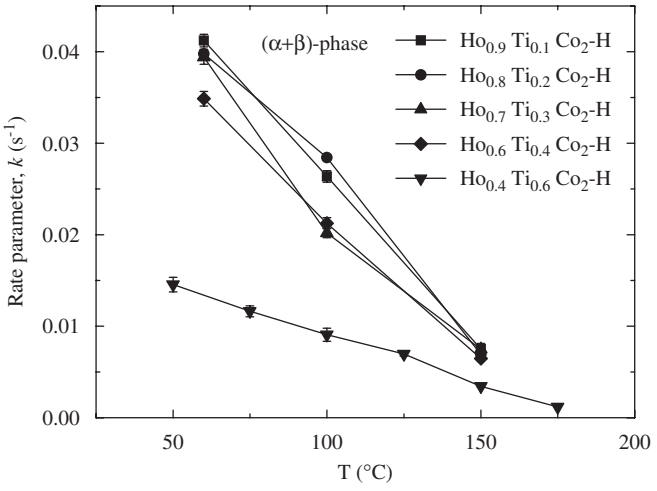

Fig. 10. Variation of rate parameter as a function of temperature at a constant initial pressure of 1 bar for $Ho_{1-x}Ti_xCo_2$-H in the $(\alpha+\beta)$-phase region.

at lower temperatures and higher pressures, the α phase could not be seen, due to the fast hydriding reaction. At higher temperatures there is no clear evidence of the β-phase formation in these experimental conditions, due to the higher equilibrium plateau pressure P_{eq}. The reaction rate parameters obtained from slopes of the straight-line segments in different regions, which represent the reaction proceeds different in different phase regions. It is observed that the values of rate parameter follows the relation $k_{(\alpha\ \text{phase})} > k_{((\alpha+\beta)\ \text{phase})} > k_{(\beta\ \text{phase})}$. Thus the reaction rate in the α phase is fast compared to the rate of H transport through the β phase.

The variation of rate parameter in the $(\alpha+\beta)$-phase region as a function of pressure and temperature is shown in Figs. 9 and 10. It is clear that the reaction rates in both phase regions are largely depending on the hydriding pressure and temperature. The rate parameters increase almost linearly with increasing hydriding pressure and follow the opposite trend with increasing temperature. In most of the cases, it can be seen that the apparent rate

parameter is independent of applied pressure and further increases with increasing temperature (i.e., thermally activated behavior), when hydrogenated at relatively higher pressures than their plateau pressures [15,16,36]. However, the rate parameter largely depends on the driving force, $P_d = P - P_{eq}$, where P is the applied pressure, when the hydriding pressure is not high relative to that of equilibrium plateau pressure. Thus the variations of reaction rates depending on the hydriding pressure and temperature in the present case are attributed to the large change in the driving force P_d. When the hydriding kinetics carried out at near equilibrium pressures, the increase in temperature would reduce the driving force ($P - P_{eq}$), since the hydrogen equilibrium pressure P_{eq} increases with the increase in temperature. The reaction rate is more sensitive to temperature in the case of low initial ($P - P_{eq}$) than that of high initial ($P - P_{eq}$). As a result, the reaction rate is slower at higher temperatures or lower hydriding pressures [3,17,37–40].

4. Conclusion

The enthalpy of hydride formation representing the hydride stability decreases with increasing Ti substitution in $Ho_{1-x}Ti_xCo_2$-H. The hydrogen absorption kinetics in $Ho_{1-x}Ti_xCo_2$-H follows the first-order-type reaction. The hydriding reaction rates of $Ho_{1-x}Ti_xCo_2$-H at various constant temperatures increase almost linearly with increasing applied pressure and follow opposite trend with temperature due to decrease in the driving force ($P - P_{eq}$).

Acknowledgments

The authors are grateful to IITM and DST, India for the financial support.

References

[1] L. Schlapbach (Ed.), Hydrogen in Intermetallic Compounds—I (Springer Topics in Applied Physics, vol. 63), Springer, Berlin, 1988.
[2] I. Jacob, D. Shaltiel, J. Less-Common Met. 65 (1979) 117.
[3] G. Srinivas, V. Sankaranarayanan, S. Ramaprabhu, Int. J. Hydrogen Energy 32 (2007) 2480.
[4] G. Srinivas, V. Sankaranarayanan, S. Ramaprabhu, J. Phys. D: Appl. Phys. 40 (2007) 1183.
[5] M. Di Chio, S. Livraghi, M. Baricco, J. Alloys Compd. 426 (2006) 180.
[6] Yuntao Wang, Huaiyu Shao, Yan Li, Lei Xie, Xingguo Li, Seiki Takahashi, J. Magn. Magn. Mater. 311 (2007) 535.
[7] I.Yu. Zavaliy, R. Cerny, V.N. Verbetsky, R.V. Denys, A.B. Riabov, J. Alloys Compd. 358 (2003) 146.
[8] G. Srinivas, V. Sankaranarayanan, S. Ramaprabhu, J. Alloys Compd. 448 (2008) 159.
[9] T.R. Kesavan, S. Ramaprabhu, K.V.S. Rama Rao, Int. J. Hydrogen Energy 25 (2000) 983.
[10] R. Ramesh, K.V.S. Rama Rao, J. Alloys Compd. 191 (1993) 101.
[11] T. Ozaki, H.B. Yang, T. Iwaki, S. Tanase, T. Sakai, H. Fukunaga, N. Matsumoto, Y. Katayama, et al., J. Alloys Compd. 408–412 (2006) 294.
[12] X.B. Yu, T. Dou, Z. Wu, B.J. Xia, J. Shen, Nanotechnology 17 (2006) 268.
[13] J. Kleperis, G. Wojcik, A. Czerwinski, J. Skowronski, M. Kopczyk, M. Beltowska-Brzezinska, J. Solid State Electrochem. 5 (2001) 229.
[14] N. Mani, S. Ramaprabhu, Int. J. Hydrogen Energy 30 (2005) 53.
[15] M. Kandavel, S. Ramaprabhu, J. Phys.: Condens. Matter 15 (2003) 7501.
[16] L. Belkbir, E. Joly, N. Gerard, J. Less-Common Met. 81 (1981) 199.
[17] M.Y. Song, M. Pezart, B. Darriet, P. Hagemuller, J. Less-Common Met. 103 (1984) 145.
[18] Q. Li, L.-J. Jiang, K.-C. Chou, Q. Lin, F. Zhan, K.-D. Xu, X.-G. Lu, J.-Y. Zhang, J. Alloys Compd. 399 (2005) 101.
[19] Q. Li, K.-C. Chou, Q. Lin, L.-J. Jiang, F. Zhan, Int. J. Hydrogen Energy 29 (2004) 1383.
[20] M. Bereznitsky, I. Jacob, J. Bloch, M.H. Mintz, J. Alloys Compd. 363 (2004) 203.
[21] X.-L. Wang, S. Suda, Int. J. Hydrogen Energy 15 (1990) 569.
[22] J. Block, J. Alloys Compd. 361 (2003) 130.
[23] G. Srinivas, V. Sankaranarayanan, S. Ramaprabhu, Mater. Sci. Eng. A 472 (2008) 293.
[24] G. Srinivas, V. Sankaranarayanan, S. Ramaprabhu, Alloys Compd 458 (2008) 574.
[25] G. Srinivas, V. Sankaranarayanan, S. Ramaprabhu, Solid State Sci 9 (2007) 973.
[26] C.E. Lundin, F.E. Lynch, C.B. Magee, J. Less-Common Met. 56 (1977) 19.
[27] M. Boulgallat, N. Gerard, O. Canet, A. Percheron-Guegan, Z. Phys. Chem. 179 (1993) 261.
[28] A. Percheron-Guegan, C. Lartigue, J.C. Achard, J. Less-Common Met. 109 (1985) 287.
[29] J.Y. Lee, C.N. Park, S.M. Pyun, J. Less-Common Met. 89 (1983) 163.
[30] Y.B. Eliyahu, M. Brill, M.H. Mintz, J. Chem. Phys. 111 (1999) 6053.
[31] P.S. Rudman, J. Less-Common Met. 89 (1983) 93.
[32] A. Karty, J. Grunzweig-Genossar, P.S. Rudman, J. Appl. Phys. 50 (1979) 7200.
[33] W. Zhang, J. Cimato, A.J. Goudy, J. Alloys Compd. 201 (1993) 175.
[34] K.R. Clay, A.J. Goudy, R.G. Schweibenz, A. Zarynow, J. Less-Common Met. 166 (1990) 153.
[35] V.K. Sinha, F. Pourarian, W.E. Wallace, J. Less-Common Met. 87 (1982) 283.
[36] N. Mani, S. Ramaprabhu, J. Alloys Compd. 363 (2004) 275.
[37] P.S. Rudman, J. Appl. Phys. 50 (1979) 7195.
[38] M.Y. Song, M. Pezart, B. Darriet, P. Hagemuller, J. Solid State Chem. 56 (1985) 191.
[39] J.Y. Lee, S.M. Byun, C.N. Park, J.K. Park, J. Less-Common Met. 87 (1982) 149.
[40] J.S. Han, J.Y. Lee, J. Less-Common Met. 131 (1987) 109.